

## FOUR SWITCHTHREE PHASE Y SOURCE INVERTER FED AC DRIVE USING FOPID CONTROLLER

K. Srinivasan<sup>1</sup>, R. Zahira<sup>2</sup>, D.Lakshmi<sup>3</sup>, B. Partheeban<sup>4</sup>, TKS. Sathyanarayanan<sup>5</sup>

<sup>1</sup>Department of EEE, Tagore Engineering College,  
Chennai, INDIA, [omsrivas@yahoo.co.in](mailto:omsrivas@yahoo.co.in)

<sup>2</sup>Department of EEE, B S Abdur Rahman Crescent Institute of Science and Technology  
Chennai, INDIA, [zahirajaved@gmail.com](mailto:zahirajaved@gmail.com)

<sup>3</sup>Dept of EEE AMET deemed to be university ,  
Chennai, INDIA, [Lakshmiec@gmail.com](mailto:Lakshmiec@gmail.com)

<sup>4</sup>Department of EEE, Tagore Engineering College,  
Chennai, INDIA, [partheeban.balakrishnan@gmail.com](mailto:partheeban.balakrishnan@gmail.com)

<sup>5</sup>Department of EEE, Tagore Engineering College,  
Chennai, INDIA, [tkssujaakil@gmail.com](mailto:tkssujaakil@gmail.com)

**Abstract**—A fractional-order PID (FOPID) controller induction motor driver with Y-source inverter is presented as a low-cost, minimized-component solution. This topology combines the advantages of the traditional 3-phase 4-switch inverter with those of the Y-source network. Besides its self-amplification properties, this topology has fewer switches and can also act as a buck converter. The FOPID controller contains five important variable coefficients. They are called proportional operator ( $K_p$ ), integral operator ( $K_i$ ), differential operator ( $K_d$ ), integral operator ( $K_i$ ), differential operator ( $K_d$ ), fractional integral operator ( $\lambda$ ) and fractional derivative ( $\mu$ ). The performance of the controller mainly depends on the chosen values of the above operators ( $K_p$ ,  $K_i$ ,  $K_d$ ,  $\lambda$ ,  $\mu$ ). One of the main goals of this article is to optimize the values of these five parameters to improve system performance. A new integrated Y-source inverter system enables drive-thru during voltage sags, reducing grid harmonics and extending the output voltage range. These new capabilities are demonstrated through analysis, simulation and experimentation

**IndexTerms**—*Embedded Controller, Harmonic distortion, four-switch three-phase inverter, y-source inverter.*

### INTRODUCTION

There are currently two converter topologies used for variable speed drives. A conventional PWM (Pulse Width Modulation) inverter and a 3-level PWM inverter with a DC-DC boost converter [1]. Traditional PWM inverter topologies place heavy loads on switches and solid-state motors, limiting the components that can control the motor's constant speed. A boost DC/DC PWM inverter topology can reduce the stress and limitations of issues such as high load and complexity associated with two-stage power conversion. A powerful way to alter the control between source and load is impedance organization in a variety of electrical power conversion applications. Although the Z source impedance arrangement was first attempted by him in DC-AC inverters, its use is not limited and has in fact been attempted in many types of voltage converters [8]. Each of these schemes has its own claims feature

which can be dealt with depending on the intended use. Therefore, it does not make sense to prefer a specific system, but to look for options that can integrate all the necessary functions. To do this, an exclusive Y source impedance network is proposed. In this paper, we present a Y source impedance network to realize a three-phase inverter with very high gain and small number of switches as shown in Figure 1.

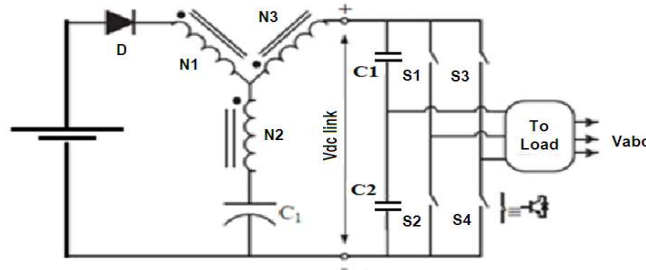


Fig. 1. System configuration using reduced switch Y source inverter.

The proposed inverter consists of a Y source network on the input side, a three-phase bridge inverter with four switches and a filter on the output side. The basic structure of the source impedance network Y consists of a subordinate diode D, a capacitor C and, above all, a transformer with three windings (N1, N2, N3) to increase the gain with a low feed percentage. The transformer is directly connected to the inverter bridge and the coupling must be tight to reduce leakage inductance in the windings. Controllers like PI have simple schemes for increasing damping, reducing extreme overshoot, decreasing bandwidth, and increasing rise time. In any case, the PI controller may not be sufficient to maintain the target motor speed in the presence of obstacles or system disturbances. As a result, other adaptive control strategies such as PID and FOPID controllers had to be used. The FOPID controller contains 5 influence coefficients. - Proportional operator ( $K_p$ ), Integral operator ( $K_i$ ), Differential operator ( $K_d$ ), Fractional integral ( $\lambda$ ) and Fractional derivative ( $\mu$ ). PID and PI controllers are known to increase the value of each parameter to 1. Since the performance of the controller depends substantially on the chosen values of the operators above ( $K_p$ ,  $K_i$ ,  $K_d$ ,  $\lambda$ ,  $\mu$ ), one of the main goal of this document is to improve them. Parameters to improve engine performance and improve and extend speed control.

**FOUR SWITCH THREE PHASE INVERTER MODEL**

In this work, the inverting switch is considered as an ideal power switch and the conduction state of the power switch should be related to the binary variables S01 to S04 [11]. A binary '1' means closed and a '0' means open. Instructions S01 to S03 and S02 to S04 are complementary and are grouped.

$$S_{03} = 1 - S_{01} \tag{1}$$

$$S_{04} = 1 - S_{02} \tag{2}$$

Also, it will be assumed that a stiff voltage is available across the two dc-link capacitors and:

$$E_{C1} = E_{C2} = E/2 \tag{3}$$

where, E corresponds to a stiff dc-link voltage, i.e., the actual value of the dc-link voltage is equal to E. The phase voltage equations of the motor can be written as a function of the switching logic of the switches and the dc-link voltage and given by [10]:

$$E_a = E_{dc}(4S_a - 2S_b - 1)/3 \tag{4}$$

$$E_b = E_{dc}(-2S_a + 4S_b - 1)/3 \tag{5}$$

$$E_c = E_{dc}(-2S_a - 2S_b + 2)/3 \tag{6}$$

Where:

$E_a, E_b, E_c$  = Inverter output voltages

$E_{dc}$  = Be the voltage across the dc-link capacitors

$S_a, S_b$  = The switching functions for each phase leg

In matrix form, the above equations can be written as:

$$\begin{bmatrix} E_a \\ E_b \\ E_c \end{bmatrix} = \frac{E_{dc}}{3} \begin{bmatrix} 4 & -2 \\ -2 & 4 \\ -2 & -2 \end{bmatrix} \begin{bmatrix} S_a \\ S_b \end{bmatrix} + \frac{E_{dc}}{3} \begin{bmatrix} -1 \\ -1 \\ 2 \end{bmatrix}$$

For a well-adjusted capacitor voltage, the four switching arrangements lead to four voltage devices. Table 1 shows the different modes of operation and the equivalent output voltage vector of the inverter.

Table 1: The four arrangements of the states of the power switches and the resultant terminal voltages  $V_a, V_b$  and  $V_c$  are given in Table 1

Table 1

$S_{01}$	$S_{02}$	$E_a$	$E_b$	$E_c$
0	0	$-U_c/6$	$-U_c/6$	$-U_c/3$
1	0	$U_c/2$	$-U_c/2$	0
1	1	$U_c/6$	$U_c/6$	$-U_c/3$
0	1	$-U_c/2$	$U_c/2$	0

**Y-SOURCE INVERTER**

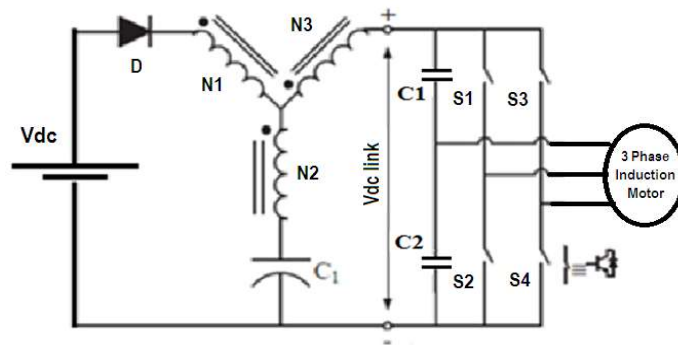


Fig. 2: Circuit of the Y-source inverter.

A Y-source inverter consists of a submissive diode, a capacitor, a three-winding tightly coupled inductor, and a three-phase bridge structure as shown in Figure 2. In the circuit, the diode expects the reverse current of the AC output current and then disconnects the load from nutrition. The capacitor acts as a DC link capacitor between the DC source and the Y network, creating a differential that draws a DC input current. The three twisted Y-coils are tightly coupled to further reduce the risk of overflow and provide high gain at low

insertion speeds. Downstream of network Y, a three-phase inverter bridge is connected to an SPWM-controlled LCL filter. LCL filters bridge the gap between the inverter output and utility networks. They cancel all the harmonics present in the output. Furthermore, the use of LCL filters reduces the dependence on network parameters. The output is not a pure sine wave due to electromagnetic noise and high switching frequency.

### Y- SOURCE INVERTER FED INDUCTION MOTOR DRIVE

The induction motor frame resists rotation in accordance with general limitations. A diode rectifier supplied by a 230 V AC line generates approximately 310 V DC on the intermediate circuit. This is typically 1.35 times the input voltage assuming overwhelming load. In a low capacitance drive with no significant inductance, the line current is discontinuous and the DC voltage is almost 1.41 times the line-to-line input voltage. A lower overall voltage limits the output power proportional to the square of the voltage. This can be a highly undesirable situation for many applications. The reason for this is that the motor and drive frame must be exceptionally large for the power required. A voltage drop can disrupt the pick-up motor drive system, shutting down the base load and the frame. DC capacitors in responsive motor drives can be relatively low power capacity components that cannot hold DC voltage above operating levels during such dips. The need for transmission capacity can become a real problem for sensitive loads driven by the drive. Measures to improve continuity were sought. Industrial drives offer the alternative of using fly-back converters or up-converters with liveliness capability to achieve drive-through. However, these choices are a compromise of approach, estimation and complexity. Inrush currents and direct current from diode rectifiers can pollute lines. Low power factor is another problem with conventional motors. Unwavering quality and design can lead to mismatches due to EMI causing overshoot, which leads to inverter destruction, destroys the dead time required to maintain a strategic distance from overshoot, and erratic operation at low speeds. It is affected by the converter design of the voltage source as it can cause common mode voltages which can also lead to hum currents and premature motor failure. The latest inverters developed recently, Y-source inverters, have a special drive frame to solve the above problems.

The FOPID is an extension of the PID controller commonly used in industrial systems. The FOPID depends on the fractional calculation and therefore guarantees a good behavior of the dynamic system and a lower sensitivity to the fluctuating components in a controlled system. A closed loop for the controller corrects the deviation between the response value and the set point to obtain the desired output. The transmission equation of the FOPID controller is as follows:-

$$G_c(s) = K_p + \frac{K_i}{s^\lambda} + K_d s^\mu$$

Five elements ((K<sub>p</sub>, K<sub>i</sub>, K<sub>d</sub>, λ, μ), as mentioned above, characterize the behavior of the fractional controller. Therefore, the relationship between conventional PI, PID and FOPID is shown in Fig. 2 (a) It is clear that the FOPID includes the conventional PI, PID in its behavior This is the case when μ is set and λ is equal to 1.

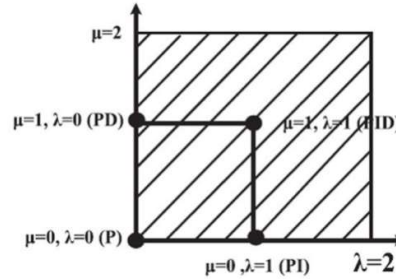


Fig. 2.(a). FOPID Controller

Overcome the above issues. FOPID is an extension of the PID controller widely used in industrial systems. Because FOPID is fractional, dynamic systems behave better and are less sensitive to changes in control system components. The controller's control loop corrects any error between the response value and the setpoint to achieve the desired output. The transfer equation for the FOPID controller is: The five elements  $((K_p, K_i, K_d, \lambda, \mu))$  characterize the behavior of the fractional controller, as already mentioned. Therefore, the relationship between the conventional PI, PID and FOPID is shown in Fig. 2(a). It is clear that FOPID integrates the conventional PI into its behavior. PID occurs when  $\mu$  and  $\lambda$  are set equal to one. This is incomprehensible with conventional pickup motor drive systems. Acceptance motor drives based on Y-source inverters can supply any breakdown voltage above line voltage, regardless of input voltage, reducing motor quality but improving factor of power without the need for additional circuitry. thus harmonic currents and common mode voltages are reduced. This article presents the implementation of a three-phase induction motor with gear reduction circuit fed by a Y-source inverter using the PIC microcontroller PIC16F84A.

## RESULTS AND DISCUSSION

To verify the feasibility of the inverter design and its control method, a computer simulation model is created using MATLAB/SIMULINK software. Figure 3 shows a fully developed Y-source with a three-phase, four-switch inverter and a closed-loop FOPID controller. The technique used to generate PWM pulses compares a sinusoidal drive voltage (at the desired output frequency and proportional to the magnitude of the output voltage) to a triangle wave at the selected switching frequency. The motor current and voltage waveform of the Y-source 3-phase 4-switch inverter assumes the same conditions as the 3-phase 6-switch inverter. It is clear that the starting current is within reasonable limits. Figure 4 shows the line voltage waveforms of a three-phase Y-source inverter with four breakers. The stationary three-phase currents in FIG. 5 approximates the regulated state of a three-phase Y-source inverter with four switches. Figure 6 shows that the motor speed of the Y source is lower when using a 3-phase inverter with 4 switches and a closed-loop FOPID controller than the PI controller. We also clearly see that the PI controller has a stronger ripple component than its FOPID controller. The Y motor torque using a three-phase inverter with four switches and a closed-loop FOPID controller is shown in FIG. Figure 8 shows the harmonic spectrum of the inverter phase current  $I_a$ . The total harmonic distortion (THD) of the three-phase quad source Y inverter controlled by FOPID is 4.22%, and the THD of the PI controller of the three-phase quad source Y inverter is 4.99%. A comparison of the time domain parameters is shown in Figure 9. A comparison of the effective THD of PI and FOPID is shown in Figure 10.

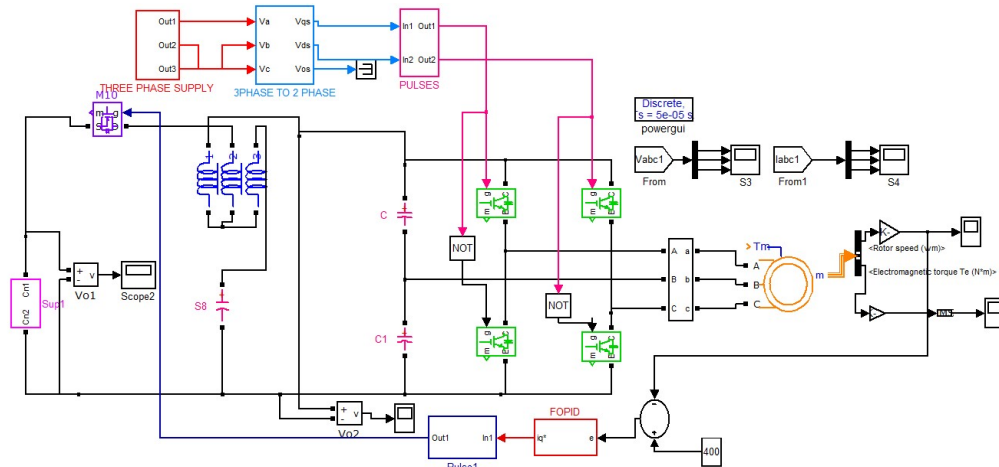


Fig.3 Circuit diagram of Y-source with four switch three phase inverter with closed loop FOPID controller

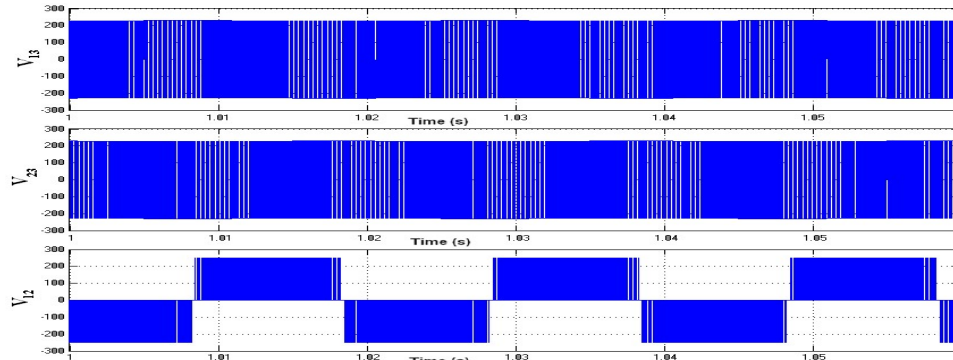


Fig. 4 Line voltage waveform of four switch three phase Y source inverter.

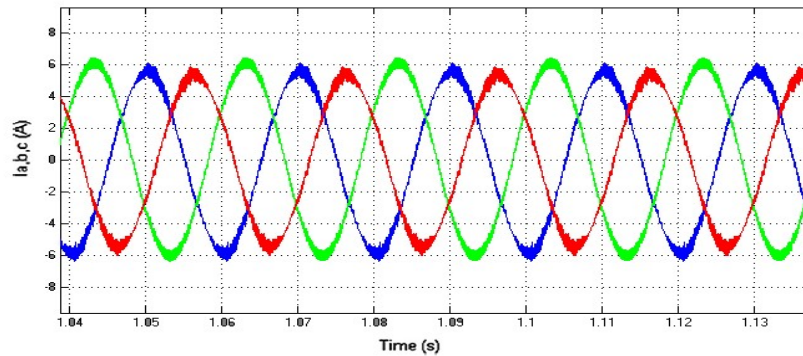


Fig 5. Three phase stator currents in the proposed method.

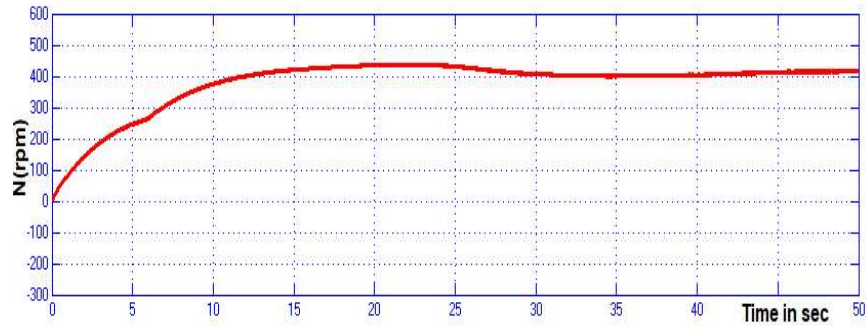


Fig.6 Motor speed of Y-source with four switch three phase inverter with closed loop FOPID controller

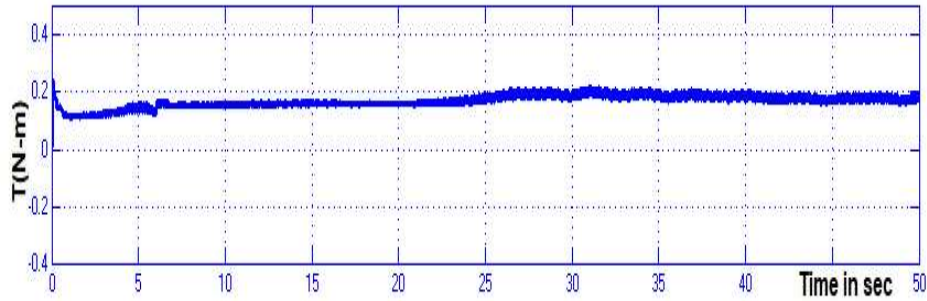


Fig.7. Motor torque of Y-source with four switch three phase inverter with closed loop FOPID controller

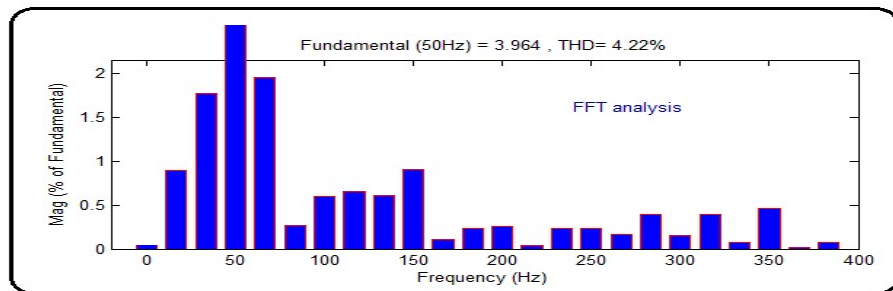


Fig.8 Output current THD of closed loop FOPID controller

Table-2 Comparison of Time Domain Parameters

Controllers	Rise time (s)	Peak time (s)	Setting time (s)	Steady state error (rpm)
PI	15	24	35	4.56
FOPID	13	20	29	2.78

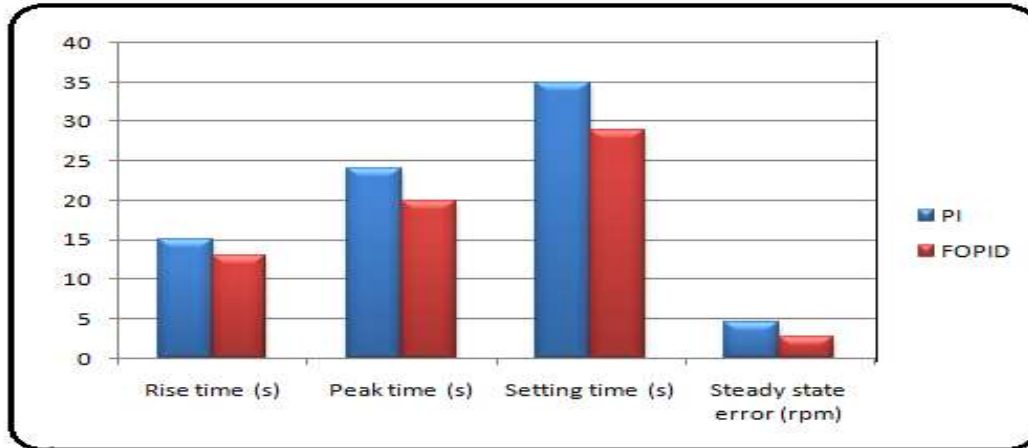


Fig.9 Comparison of Time Domain Parameters

Table-3 Comparison of output current THD

Controllers	Current THD (%)
PI	4.91
FOPID	4.22

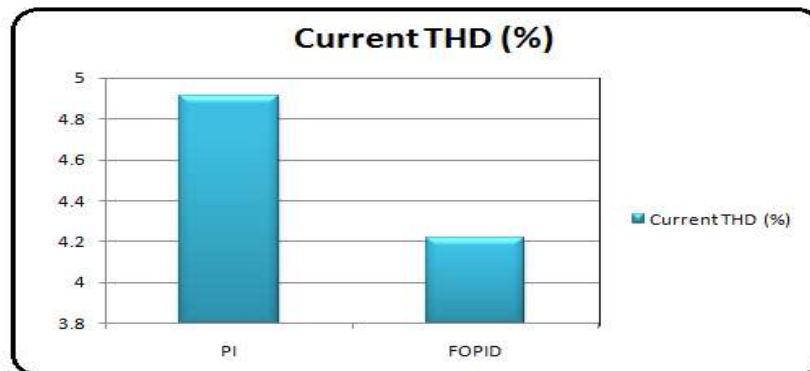


Fig.10 Comparison of current THD of PI and FOPID

The validity of the Y-source inverter is evidenced by the absence of overshoot and undershoot in the speed response and steady-state errors. From Figures 6 and 8, it can be seen that the speed response and harmonic distortion of the IM drive is based on a 3-phase 4-switch Y-inverter. It was found that the reduced switching action of the Y-source 3-phase inverter is very close to the control of a traditional 6-switch 3-phase inverter. Studies and replicas show that this inverter can greatly reduce the complexity of control calculations and reduce their costs.

## EXPERIMENTAL RESULTS

For preliminary approval of a proposed Y-source inverter with built-in controlled switches to drive an induction motor, a model was built using MOSFETs as switching devices, and the test load could be three-phase (wound rotor, 0.5 PS ). This is shown in Figure 11. In this article, the



hardware is implemented using a PIC16F84A microcontroller IC. The main problem with PIC microcontrollers is that the instruction set of this controller is smaller than that of normal microcontrollers. It is far from conventional processors designed primarily for Complex Instruction Set Computer (CISC). Tuning a RISC processor to a CISC processor is RISC information, not too difficult and results in faster performance. RISC processors require one clock per instruction, while CISC processors require multiple clocks per instruction. Translation becomes an intensive task because CISC controllers are constantly updated by microcode, which is much slower than computers running RISC. A PIC16F84A microcontroller is used to generate the MOSFET start pulse. Used to control inverter output. Microcontrollers have advantages over analog circuits and small processors, such as fast response, low occupancy, and small size. Drivers are also known as power amplifiers because their purpose is to increase the clock performance of a microcontroller. They are also called optocoupler integrated circuit. The microcontroller and the control circuit are separated from each other. The PIC16F84A belongs to its mid-range family of PIC microcontrollers. Each 14-bit word of program memory is the same width as each device instruction, so the program memory contains 1K words decoded into 1024 pieces of information. The information memory (RAM) consists of 68 bytes. The information EEPROM consists of 64 bytes. Figure 12. shows the experimental phase load voltages of the proposed inverter.

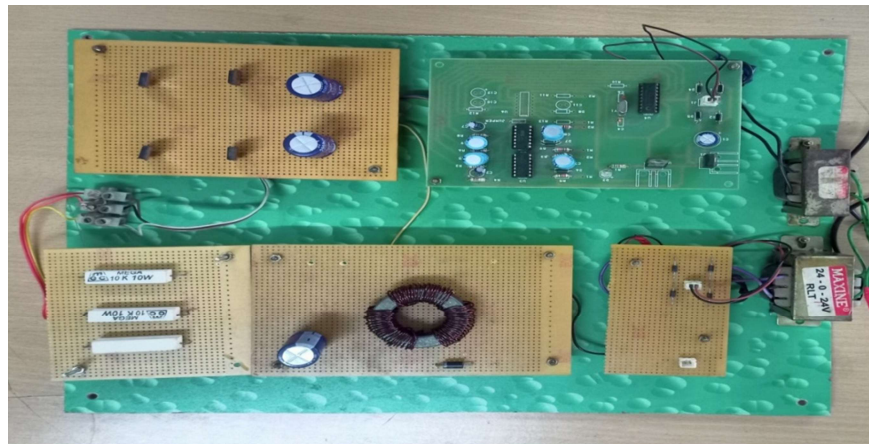


Fig. 11 Four switch three phase Y source inverter fed induction motor drive prototype.

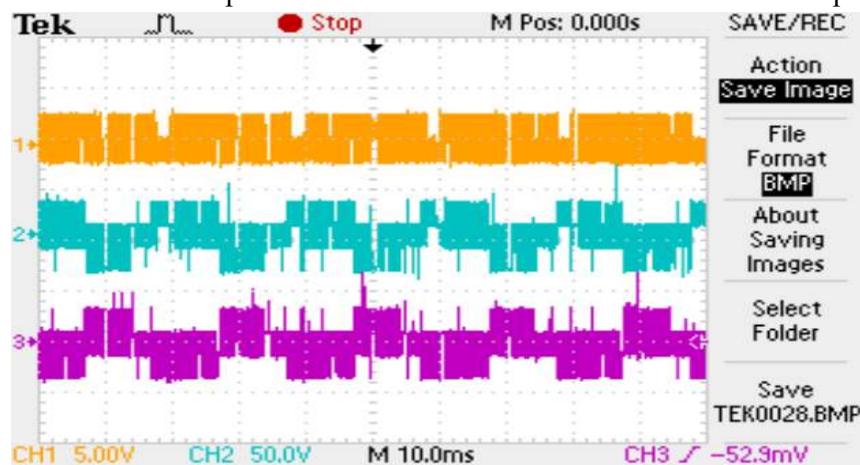


Fig.12. Phase load voltages

## CONCLUSION

The study explains that a three-phase, 4-switch, Y-source inverter topology has become a better option for innovation than traditional inverters because it is more efficient, more reliable and requires less investment in the conversion system. The working principle and analysis have been verified by simulations of actual harmonic content and experimental results to confirm operation and validate promising highlights. Apart from that, its 3-phase, 4-switch, Y-source inverter ASD structure has unique advantages such as zero and harmonic currents that make it very attractive for many ASD applications. We obtain survey results that agree very well with the simulation results. You can increase input voltage, increase efficiency, and minimize component count to reduce costs.

## References

- [1]. Xue, Y., Chang, L., Baekhj, Kjaer, S., Bordonau, J. and Shimizu, T., "Topologies of singlephase inverters for small distributed power generators: an overview" IEEE Trans. on Power Electronics, vol.19, pp. 1305-1314, Sept. 2004.
- [2]. M. Calais, J. Myrzik, T. Spooner and V. G. Agelidis, "Inverters for single-phase grid connected photovoltaic systems – an overview," Proc. IEEE Power Electronics Specialists Conference, PESC, 2002, pp. 1995-2000.
- [3]. Hong Mao and Osama Abdel –Rahman and IssaBatarseh:"Active resonant tank to achieve zero voltage switching for non isolated DC-DC converters with synchronous rectifiers". IEEE IECON2005,pp.585-591(2005)
- [4]. A.Kotsopoulos and D.G.Holmes,"Performance of a series –parallel resonant DC-DC converter module for high current low voltage applications",IEE PEDEDS1998,2,pp.861-866(1998).
- [5]. S.B.Kjaer,J.K.Pedersen,F.Blaabjerg, "A Review of Single-Phase Grid-Connected Inverters for Photovoltaic Modules" IEEE Trans. On Industrial Applications, vol.41, no.5, September/October 2005.
- [6]. R.O.Caceres, I.Barbi "A boost DC-AC converter, analysis, design and experimentation" IEEE Trans. On Power Electronics, vol.14, no.1, January 1999.
- [7]. K. Ogura, T. Nishida, E. Hiraki and M. Nakaoka, Shinichiro Nagai, "Timesharing Boost Chopper Cascaded Dual Mode Single-phase Sine wave Inverter for Solar Photovoltaic Power Generation System" Proc. Of 35th Annual IEEE Power Electronics Specialists Conference Aachen, Germany, 2004, pp.4763-4767.
- [8]. Wang, W.; Luo, A.; Xu, X.Y.; Fang, L.; Thuyen, C.M.; Li, Z. Space vector pulse-width modulation algorithm and DC-side voltage control strategy of three-phase four-switch active power filters. IET Power Electron. **2013**, 6, 125–135.
- [9]. Dasgupta, S.; Mohan, S.N.; Sahoo, S.K.; Panda, S.K. Application of four-switch-based three-phase grid-connected inverter to connect renewable energy source to a generalized unbalanced microgrid system. IEEE Trans. Ind. Electron. **2013**, 60, 1204–1215.
- [10]. Freire, N.M.A.; Marques Cardoso, A.J. A Fault-Tolerant Direct Controlled PMSG Drive for Wind Energy

- Conversion Systems. *IEEE Trans. Power Electron.* **2014**, 61, 821–834.
- [11]. Fadil, H.; Driss, Y.; AiteDriss, Y.; Elafyani, M.L.; Abd Rahim, N. Sliding-Mode Speed Control of PMSM with Fuzzy-Logic Chattering Minimization—Design and Implementation. *Information* **2015**, 6, 432–442.
- [12]. Trinh, Q.-N.; Lee, H.-H. Low Cost and High Performance UPQC with Four-Switch Three-Phase Inverters. *J. Electr. Eng. Technol.* **2015**, 10, 1015–1024.
- [13]. Hu, Y.; Gan, C.; Cao, W.; Li, W. Central-Tapped Node Linked Modular Fault Tolerance Topology for SRM Based EV/HEV Applications. *IEEE Trans. Power Electron.* **2016**, 31, 1541–1554.
- [14]. Zeng, Z.Y.; Zheng, W.Y.; Zhao, R.X.; Zhu, C.; Yuan, Q.W. Modelling modulation and control of the three-phase four-switch PWM rectifier under balanced voltage. *IEEE Trans. Power Electron.* **2016**, 31, 4892–4905.
- [15]. Zeng, Z.; Zheng, W.; Zhao, R. Performance Analysis of the Zero-Voltage Vector Distribution in Three-Phase Four-Switch Converter Using a Space Vector Approach. *IEEE Trans. Power Electron.* **2017**, 9, 1732–1740.